Communication: Distinguishing between bulk and interface-enhanced crystallization in nanoscale films of amorphous solid water

Chunqing Yuan, R. Scott Smith, and Bruce D. Kay

Citation: J. Chem. Phys. **146**, 031102 (2017); doi: 10.1063/1.4974492
View online: http://dx.doi.org/10.1063/1.4974492
View Table of Contents: http://aip.scitation.org/toc/jcp/146/3
Published by the American Institute of Physics

Communication: Distinguishing between bulk and interface-enhanced crystallization in nanoscale films of amorphous solid water

Chunqing Yuan, R. Scott Smith,[a] and Bruce D. Kay[a]
Physical Sciences Division, Pacific Northwest National Laboratory, Richland, Washington 99352, USA

(Received 6 December 2016; accepted 9 January 2017; published online 20 January 2017)

The crystallization of amorphous solid water (ASW) nanoscale films was investigated using reflection absorption infrared spectroscopy. Two ASW film configurations were studied. In one case the ASW film was deposited on top of and capped with a decane layer ("sandwich" configuration). In the other case, the ASW film was deposited on top of a decane layer and not capped ("no cap" configuration). Crystallization of ASW films in the "sandwich" configuration is about eight times slower than in the "no cap." Selective placement of an isotopic layer (5% D_2O in H_2O) at various positions in an ASW (H_2O) film was used to determine the crystallization mechanism. In the "sandwich" configuration, the crystallization kinetics were independent of the isotopic layer placement whereas in the "no cap" configuration the closer the isotopic layer was to the vacuum interface, the earlier the isotopic layer crystallized. These results are consistent with a mechanism whereby the decane overlayer suppresses surface nucleation and provide evidence that the observed ASW crystallization in "sandwich" films is the result of uniform bulk nucleation. *Published by AIP Publishing.* [http://dx.doi.org/10.1063/1.4974492]

The properties of amorphous solid water (ASW) are of interest for a variety of reasons including its use as a model system for studying supercooled liquid water, amorphous materials, and water in astrophysical environments.[1–9] While not found naturally on earth, it can be created by vapor deposition onto a cold substrate ($T < 130$ K) in the laboratory.[5,10] The vapor deposited solid is metastable and will eventually transform into the crystalline phase when heated to higher temperatures (typically greater than 130 K), where of course, the kinetics of the crystallization will depend on the temperature.

One motivation for many of these studies is to use the ASW films to extract the nucleation and growth parameters for the formation of crystalline ice from deeply supercooled liquid water.[11–15] The idea is that when ASW is heated above its glass transition, it will transform into a supercooled liquid prior to crystallization. The crystallization kinetics will provide information about the properties of supercooled liquid water. A variety of experimental techniques (including desorption,[16–20] physisorption,[11,21–24] infrared spectroscopy,[5,10,25–28] and electron microcopy[12,29]) have been used to study ASW crystallization. The majority of the above mentioned studies report that crystallization occurs via bulk nucleation although a few studies suggest that nucleation may start at the vacuum interface.[24,30]

In recent work studying crack formation in ASW films, it was observed that the crack formation begins at the ASW/vacuum surface.[31–33] Because crack formation is believed to accompany crystallization,[34,35] in a follow-up study temperature programmed desorption (TPD) and reflection absorption infrared spectroscopy (RAIRS) were employed to measure surface and bulk crystallization directly.[36] Those results clearly showed that the crystallization of ASW films in vacuum proceeds via a "top-down" mechanism. In the proposed mechanism, nucleation begins at the ASW/vacuum interface resulting in crystallization of the outer surface of the film. The outer crystalline layer acts as a template that results in a crystallization growth front that propagates into the bulk. Based on these results, it is likely that many prior ASW crystallization studies were the result of surface and not bulk nucleation. In the present letter, we use ASW films sandwiched between decane layers to inhibit interface nucleation and to observe bulk ASW crystallization kinetics that are the result of bulk nucleation.

The experiments were performed in an ultra-high vacuum system (UHV) that has been described in detail previously,[20,37] and only a high level description of the experiment is provided here. Briefly, the UHV chamber has a base pressure of $<10^{-10}$ Torr and the water films were deposited on a graphene-covered 1 cm diameter Pt(111) substrate. The substrate was cooled by a closed cycle helium cryostat and resistively heated by two tantalum wires spot welded to the backside of the Pt(111). The graphene layer was formed by impinging a beam of decane on the Pt substrate heated to 1100 K to form a single layer on the surface.[38] The temperature was measured by a K-type thermocouple spot-welded to the back. The temperature was measured with a precision of better than ±0.01 K and the absolute temperature was calibrated to have an accuracy of ±2 K.

The composite decane and ASW (both pure H_2O and 5% D_2O in H_2O) films were created by deposition using a quasi-effusive molecular beam at normal incidence and at a substrate temperature of ~30 K. After creation of a composite film, the substrate was heated via a linear temperature ramp

[a]Authors to whom correspondence should be addressed. Electronic addresses: Scott.smith@pnnl.gov and Bruce.Kay@pnnl.gov

(1 K/s) to and then held at the isothermal temperature of interest. The RAIRS spectra were recorded with a Bruker Vertex 70 Fourier transform infrared spectrometer where the infrared beam was incident on the sample at an angle of 82° ± 1° from normal. The infrared spectra were acquired with a resolution of 8 cm^{-1}.

Figure 1 displays a series of RAIRS spectra for a 1000 ML ASW film in a "sandwich" configuration (described below). The film was deposited at 30 K and then heated to and held at 150 K. A 5% D_2O in H_2O liquid solution was used to grow the ASW films. In the solution, D_2O reacts with H_2O to form HDO. The use of HDO facilitates the observation and analysis of ASW crystallization because the O-D stretching frequency is decoupled from the OH stretch.[39,40] This is demonstrated in Figure 1 which shows that the initial broad amorphous spectrum (red curve) eventually transforms into a relatively sharp crystalline spectrum (blue curve) with a peak at ~2426 cm^{-1}. The set of spectra have an isosbestic point, which is indicative of a transformation from one state (amorphous) to another (crystalline). The crystallization kinetics are obtained by analyzing the time series of spectra. In this work the fraction-crystallized versus time was obtained by least-squares fitting the intermediate spectra (black curves) to a linear combination of the initial 100% amorphous (red curve) and the final 100% crystalline (blue curve) spectra. Because the spectra are temperature dependent, 100% amorphous and 100% crystalline basis spectra were obtained at the temperature of each isothermal experiment and used in the analysis.

Figure 2 displays the fraction-crystallized versus time curves for 1000 ML ASW films in two configurations. Figure 2(a) displays the results for a series of isothermal experiments from 148 to 160 K where the ASW films were deposited on top of and capped with a 50 ML decane layer, which we refer to as the "sandwich" configuration. Figure 2(b) displays the results for a series of isothermal experiments from 140 to 150 K where the ASW films were deposited on top of a 50 ML decane layer but not capped, which we refer to as the "no cap" configuration. The results for both configurations show that the fraction-crystallized curves have a sigmoidal shape and that the onset time for crystallization increases with decreasing temperature. The sigmoidal behavior and the delayed onset are characteristic of nucleation and growth kinetics.[41,42]

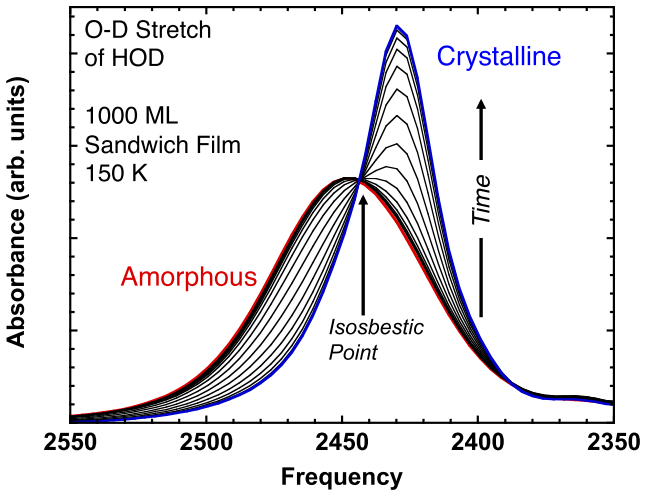

FIG. 1. A time series of RAIRS spectra obtained from a 1000 ML thick ASW film (5% D_2O in H_2O) deposited at 30 K and then heated to and held at 150 K. Displayed is the O-D stretching region for HOD. The red curve is the spectrum from a 100% amorphous film and the blue curve is the spectrum from a 100% crystalline film. The time difference between the amorphous (red curve) and crystalline (blue curve) spectra is about 3500 s.

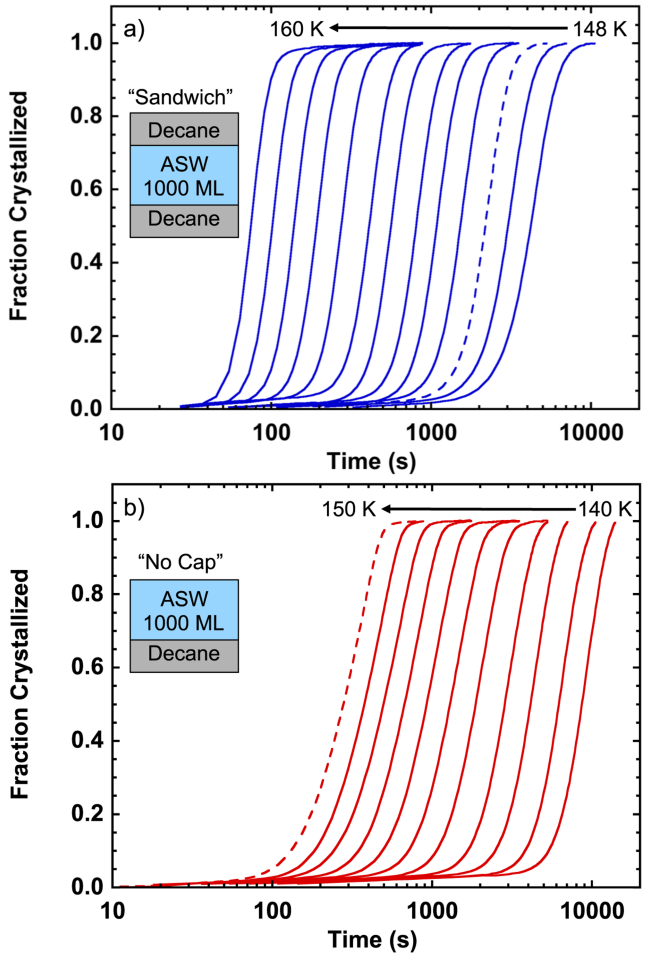

FIG. 2. Fraction-crystallized versus time curves, $x(t)$, obtained for 1000 ML ASW (5% D_2O in H_2O) films. (a) Results for films deposited between two 50 ML decane layers ("sandwich") at a series of isothermal temperatures (148–160 K). (b) Results for films deposited on top of 50 ML of decane ("no cap") at a series of isothermal temperatures (140–150 K). The dashed curves are the $x(t)$ curves for the 150 K experiments.

One difference in the results for the two configurations is that crystallization rates in the "sandwich" films are much slower than for the "no cap" films. For example, the two dashed curves in Figure 2 are both for isothermal experiments at 150 K. In the "sandwich" film the crystallization half-time, $t_{1/2}$, is ~2200 s whereas in the "no cap" film the $t_{1/2}$ is ~275 s. Clearly, the addition of the decane layer on top of the ASW film has dramatically affected the crystallization kinetics.

To obtain insight into the crystallization mechanism, experiments where an isotopic layer (5% D_2O in H_2O) was placed at various positions in the film were performed. The results for both the "sandwich" and "no cap" configurations are displayed in Figure 3(a). In these experiments (see schematics

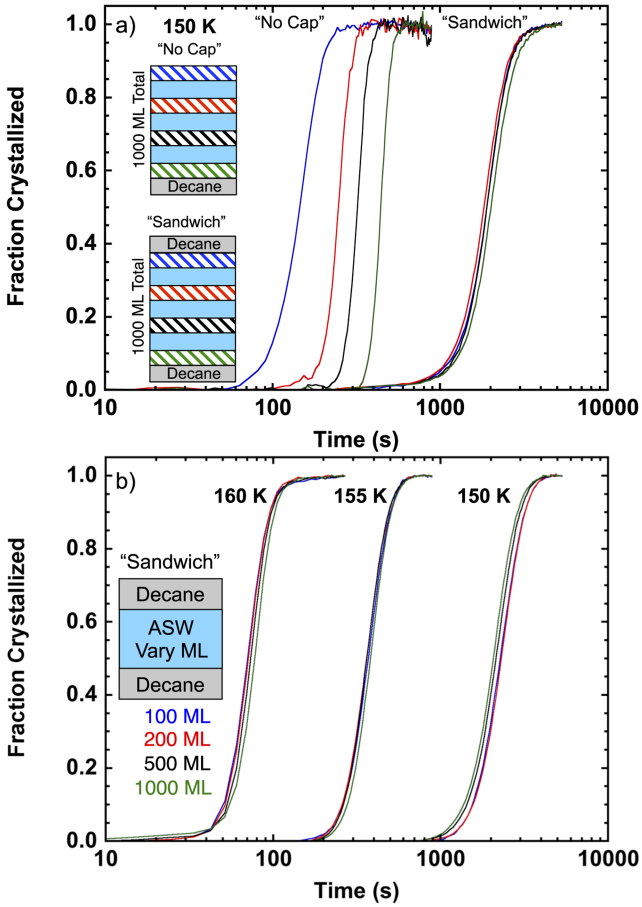

FIG. 3. (a) Fraction-crystallized of the isotopic layer versus time, $x(t)$, curves obtained from isothermal RAIRS experiments at 150 K where a 100 ML ASW layer (5% D_2O in H_2O) was placed at various positions in H_2O films in both "no cap" and "sandwich" configurations. The total thickness of the composite films was 1000 ML. The 100 ML isotopic layer was placed at the top (blue curves), 300 ML below the top (red curves), 600 ML below the top (black curves), and at the bottom (green curves) of the 1000 ML composite films. (b) Fraction-crystallized versus time, $x(t)$, curves obtained from RAIRS experiments in a "sandwich" configuration for film thicknesses of 100 ML (blue curves), 200 ML (red curves), 500 ML (black curves), and 1000 ML (green curves) at isothermal temperatures of 150, 155, and 160 K.

in Figure 3), 1000 ML ASW films were created with 900 ML of H_2O and a 100 ML isotopic layer (5% D_2O in H_2O) placed at top of the film (blue curves), 300 ML below the top (red curves), 600 ML below the top (black curves), and at the bottom (green curves). The results for the "no cap" films show that the fraction-crystallized of the isotopic layer curves shift to longer times as the 5% D_2O layer is placed farther away from the top of the film. The "no cap" results are consistent with our prior work,[36] which showed that the crystallization front propagates from the ASW/vacuum interface into the bulk. In this case, the crystallization of the isotopic layer is delayed until the crystallization front reaches the layer. In contrast, the results for the "sandwich" films show that the fraction-crystallized of the isotopic layer curves are largely independent of the 5% D_2O layer's position in the film. This means that there is no crystallization front propagation in the film. Similar results were observed for experiments at other isothermal temperatures (not shown). The "sandwich" results suggest that crystallization is occurring uniformly throughout the film.

Further evidence for a uniform crystallization mechanism in "sandwich" films is provided by experiments where the overall thickness of the ASW layer was varied. Figure 3(b) displays the fraction-crystallized versus time curves for ASW films (5% D_2O in H_2O) in a "sandwich" configuration for thicknesses of 100 (blue curves), 200 (red curves), 500 (black curves), and 1000 ML (green curves). The isothermal experiments for these thicknesses were performed at temperatures of 150, 155, and 160 K. The results show that at a given temperature, the crystallization kinetics are independent of the film thickness from 100 to 1000 ML for ASW films in the "sandwich" configuration.

Figure 4 is an Arrhenius plot of the crystallization half-times, $t_{1/2}$, for the "sandwich" (solid blue circles) and "no-cap" (solid red circles) fraction-crystallized curves in Figure 2. The data show that the $t_{1/2}$ values for the "sandwich" films are almost an order of magnitude slower that those for the "no cap" films. For example, at 149 K the $t_{1/2}$ is ~8 times longer in the "sandwich" than in the "no cap" film. The dashed lines are Arrhenius fits that yielded apparent activation energies of 67 ± 2 kJ/mol for the "sandwich" and 60 ± 2 kJ/mol for the "no cap" experiments. Obviously, a comparison of the $t_{1/2}$ values is overly simplistic and a more rigorous analysis is needed to get meaningful activation energies for specific kinetic processes. However, the lower activation energy for the "no cap" films is likely due to the apparent activation being more dominated by the growth kinetics, which are reported to have an activation energy of ~56 kJ/mol.[22] Both the differences in the $t_{1/2}$ values and the apparent activation energies between the "sandwich" and "no cap" experiments suggest that the crystallization mechanisms are different for the two configurations.

The question of whether nucleation begins at the surface or in the bulk has important implications for determining homogeneous nucleation rates in supercooled liquid

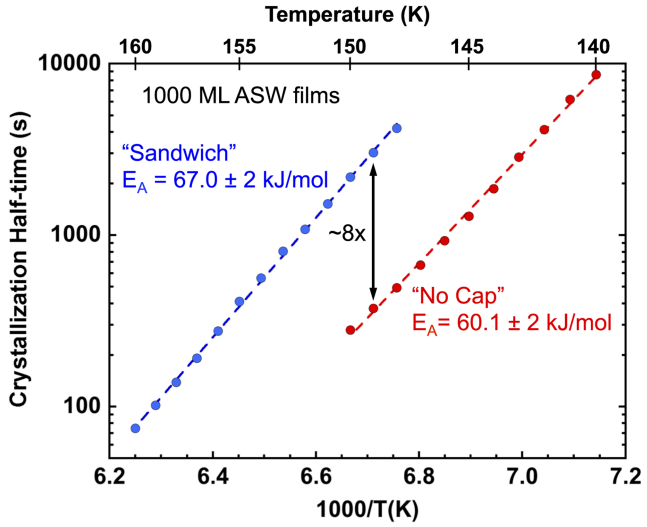

FIG. 4. Arrhenius plot of the crystallization half-times, $t_{1/2}$, for the "sandwich" and "no cap" experiments displayed in Figure 2. At 149 K the $t_{1/2}$ is ~8 times longer in the "sandwich" than in the "no cap" film. The dashed lines are Arrhenius fits that yield apparent activation energies (E_A) of 67 ± 2 kJ/mol for the "sandwich" and 60.1 ± 2 kJ/mol for the "no cap" experiments. Due to compensation effects, equally good fits can be obtained for a range of any individual Arrhenius fit parameters. The error estimate for the activation energy is the least squares fit error.

water.[6,13–15,43–49] Most experiments measure the crystallization kinetics and then extract the nucleation rate from the crystallization rate data. However, this can be complicated by the fact that crystallization of supercooled liquid water involves both nucleation and growth components. Deconvolution of the nucleation and growth rates requires knowledge of the crystallization mechanism.

Recent theoretical studies have reported conflicting evidence for the crystallization mechanism of supercooled liquid water. Some studies have argued that crystallization begins at the liquid-vapor interface or free surface interface.[15,44,45] These results are explained by the higher free volume and lower density at the interface compared to the bulk which allows for the formation of larger water clusters and eventually nuclei formation. Conversely, others have reported that nucleation begins in the bulk.[43,47] In this case the argument is that disorder and under-coordination of water molecules at the surface slows the rate of nuclei formation.

The experimental results presented here clearly show that the crystallization kinetics of the melt of ASW depends on the availability of a "free" surface. The data in Figures 2 and 4 show that the presence of a decane layer on top of the ASW film dramatically decreases the crystallization rate. In addition to decreasing the overall rate, the decane layer also affects the crystallization mechanism. This is shown in Figure 3 where the crystallization of "no cap" films is shown to proceed via a "top-down" mechanism whereas "sandwich" films crystallize uniformly and the kinetics are independent of the film thickness. Additional evidence for different crystallization mechanisms is given in Figure 4 where both the crystallization and the apparent activation energies are different for the two film configurations. In our experiments, the presence of a decane overlayer acts to limit both the available free volume and the mobility of the surface layer and this may account for the elimination of surface-induced crystallization. Another possibility is that specific interfacial interactions between the ASW surface and the decane layer may play a role. Future experiments with different adlayers (hydrophilic and hydrophobic) may be able to address this question.

These results support a model where the crystallization of ASW films in the "sandwich" configuration occurs via a bulk nucleation mechanism. Analysis of the crystallization kinetics of ASW films in a "sandwich" configuration should allow for the determination of kinetic parameters (nucleation and growth rates) that can be related to the bulk properties of deeply supercooled liquid water. The use of "sandwich" layers eliminates the contributions of nucleation at the vacuum and substrate interfaces to the observed crystallization kinetics. The extraction of the nucleation and growth parameters from the crystallization kinetics will require additional experiments and more detailed kinetic modeling that explicitly treat the interfacial and bulk nucleation and growth kinetics. Future work will employ crystalline ice templates to measure growth rates that are independent of nucleation.[50] These growth rates can then be used in kinetic simulations of the experimental crystallization kinetics to extract both the bulk and interfacial nucleation rates. The results of these combined experimental and kinetic modeling studies will be presented in a future publication.

This work was supported by the US Department of Energy (DOE), Office of Science, Office of Basic Energy Sciences, Division of Chemical Sciences, Geosciences, and Biosciences. The research was performed using EMSL, a national scientific user facility sponsored by DOE's Office of Biological and Environmental Research and located at Pacific Northwest National Laboratory, which is operated by Battelle for the DOE.

[1] P. G. Debenedetti, *Metastable Liquids: Concepts and Principles* (Princeton University Press, Princeton, N.J., 1996).
[2] P. G. Debenedetti, J. Phys.: Condens. Matter **15**, R1669 (2003).
[3] C. A. Angell, Annu. Rev. Phys. Chem. **55**, 559 (2004).
[4] C. A. Angell, Science **319**, 582 (2008).
[5] R. S. Smith, N. G. Petrik, G. A. Kimmel, and B. D. Kay, Acc. Chem. Res. **45**, 33 (2012).
[6] K. Amann-Winkel, R. Bohmer, F. Fujara, C. Gainaru, B. Geil, and T. Loerting, Rev. Mod. Phys. **88**, 011002 (2016).
[7] M. P. Collings, M. A. Anderson, R. Chen, J. W. Dever, S. Viti, D. A. Williams, and M. R. S. McCoustra, Mon. Not. R. Astron. Soc. **354**, 1133 (2004).
[8] D. A. Williams, W. A. Brown, S. D. Price, J. M. C. Rawlings, and S. Viti, Astron. Geophys. **48**, 25, doi:10.1111/j.1468-4004.2007.48125.x (2007).
[9] D. J. Burke and W. A. Brown, Phys. Chem. Chem. Phys. **12**, 5947 (2010).
[10] R. S. Smith, J. Matthiesen, J. Knox, and B. D. Kay, J. Phys. Chem. A **115**, 5908 (2011).
[11] D. J. Safarik and C. B. Mullins, J. Chem. Phys. **121**, 6003 (2004).
[12] P. Jenniskens and D. F. Blake, Astrophys. J. **473**, 1104 (1996).
[13] H. Laksmono, T. A. McQueen, J. A. Sellberg, N. D. Loh, C. Huang, D. Schlesinger, R. G. Sierra, C. Y. Hampton, D. Nordlund, M. Beye, A. V. Martin, A. Barty, M. M. Seibert, M. Messerschmidt, G. J. Williams, S. Boutet, K. Arnann-Winkel, T. Loerting, L. G. M. Pettersson, M. J. Bogan, and A. Nilsson, J. Phys. Chem. Lett. **6**, 2826 (2015).
[14] T. S. Li, D. Donadio, G. Russo, and G. Galli, Phys. Chem. Chem. Phys. **13**, 19807 (2011).
[15] T. S. Li, D. Donadio, and G. Galli, Nat. Commun. **4**, 1887 (2013).
[16] P. Lofgren, P. Ahlstrom, D. V. Chakarov, J. Lausmaa, and B. Kasemo, Surf. Sci. **367**, L19 (1996).
[17] P. Lofgren, P. Ahlstrom, J. Lausma, B. Kasemo, and D. Chakarov, Langmuir **19**, 265 (2003).
[18] N. J. Sack and R. A. Baragiola, Phys. Rev. B **48**, 9973 (1993).
[19] R. J. Speedy, P. G. Debenedetti, R. S. Smith, C. Huang, and B. D. Kay, J. Chem. Phys. **105**, 240 (1996).
[20] R. S. Smith, T. Zubkov, and B. D. Kay, J. Chem. Phys. **124**, 114710 (2006).
[21] Z. Dohnalek, R. L. Ciolli, G. A. Kimmel, K. P. Stevenson, R. S. Smith, and B. D. Kay, J. Chem. Phys. **110**, 5489 (1999).
[22] Z. Dohnalek, G. A. Kimmel, R. L. Ciolli, K. P. Stevenson, R. S. Smith, and B. D. Kay, J. Chem. Phys. **112**, 5932 (2000).
[23] D. J. Safarik, R. J. Meyer, and C. B. Mullins, J. Chem. Phys. **118**, 4660 (2003).
[24] E. H. G. Backus, M. L. Grecea, A. W. Kleyn, and M. Bonn, Phys. Rev. Lett. **92**, 236101 (2004).
[25] W. Hage, A. Hallbrucker, E. Mayer, and G. P. Johari, J. Chem. Phys. **100**, 2743 (1994).
[26] W. Hage, A. Hallbrucker, E. Mayer, and G. P. Johari, J. Chem. Phys. **103**, 545 (1995).
[27] T. Kondo, H. S. Kato, M. Bonn, and M. Kawai, J. Chem. Phys. **127**, 094703 (2007).
[28] T. Kondo, H. S. Kato, M. Bonn, and M. Kawai, J. Chem. Phys. **126**, 181103 (2007).
[29] P. Jenniskens and D. F. Blake, Science **265**, 753 (1994).
[30] E. H. G. Backus and M. Bonn, J. Chem. Phys. **121**, 1038 (2004).
[31] R. A. May, R. S. Smith, and B. D. Kay, J. Phys. Chem. Lett. **3**, 327 (2012).
[32] R. A. May, R. S. Smith, and B. D. Kay, J. Chem. Phys. **138**, 104501 (2013).
[33] R. A. May, R. S. Smith, and B. D. Kay, J. Chem. Phys. **138**, 104502 (2013).
[34] R. S. Smith, C. Huang, E. K. L. Wong, and B. D. Kay, Phys. Rev. Lett. **79**, 909 (1997).

[35]P. Ayotte, R. S. Smith, K. P. Stevenson, Z. Dohnalek, G. A. Kimmel, and B. D. Kay, J. Geophys. Res. Planets **106**, 33387, doi:10.1029/2000JE001362 (2001).
[36]C. Yuan, R. S. Smith, and B. D. Kay, Surf. Sci. **652**, 350 (2016).
[37]T. Zubkov, R. S. Smith, T. R. Engstrom, and B. D. Kay, J. Chem. Phys. **127**, 184707 (2007).
[38]G. A. Kimmel, J. Matthiesen, M. Baer, C. J. Mundy, N. G. Petrik, R. S. Smith, Z. Dohnalek, and B. D. Kay, J. Am. Chem. Soc. **131**, 12838 (2009).
[39]M. Fisher and J. P. Devlin, J. Phys. Chem. **99**, 11584 (1995).
[40]J. P. Devlin, J. Geophys. Res. Planets **106**, 33333, doi:10.1029/2000JE001301 (2001).
[41]C. N. R. Rao and K. J. Rao, *Phase Transitions in Solids* (McGraw-Hill, New York, 1978).
[42]R. H. Doremus, *Rates of Phase Transformations* (Academic Press, New York, 1985).
[43]L. Vrbka and P. Jungwirth, J. Phys. Chem. B **110**, 18126 (2006).
[44]A. Y. Zasetsky, R. Remorov, and I. M. Svishchev, Chem. Phys. Lett. **435**, 50 (2007).
[45]T. S. Li, D. Donadio, and G. Galli, J. Chem. Phys. **131**, 224519 (2009).
[46]T. S. Li, D. Donadio, L. M. Ghiringhelli, and G. Galli, Nat. Mater. **8**, 726 (2009).
[47]Y. J. Lu, X. X. Zhang, and M. Chen, J. Phys. Chem. B **117**, 10241 (2013).
[48]J. A. Sellberg, C. Huang, T. A. McQueen, N. D. Loh, H. Laksmono, D. Schlesinger, R. G. Sierra, D. Nordlund, C. Y. Hampton, D. Starodub, D. P. DePonte, M. Beye, C. Chen, A. V. Martin, A. Barty, K. T. Wikfeldt, T. M. Weiss, C. Caronna, J. Feldkamp, L. B. Skinner, M. M. Seibert, M. Messerschmidt, G. J. Williams, S. Boutet, L. G. M. Pettersson, M. J. Bogan, and A. Nilsson, Nature **510**, 381 (2014).
[49]A. Haji-Akbari and P. G. Debenedetti, Proc. Natl. Acad. Sci. U. S. A. **112**, 10582 (2015).
[50]Y. Xu, N. G. Petrik, R. S. Smith, B. D. Kay, and G. A. Kimmel, Proc. Natl. Acad. Sci. U. S. A. **113**, 14921 (2016).